Localization of Narrow Bipolar Events over Sumatra Island Based on VHF Interferometer and Magnetic Direction Finder Systems

Muhammad Zuhair Bolqiah Edris[a], Mohd Riduan Ahmad[a], Nik Mohd Zarifie Hashim[b], Shamsul Ammar Shamsul Baharin[a], Sani Irwan Salim[b], Masrullizam Bin Mat Ibrahim[b], Mohd Zafri Baharuddin[c], Yuji Takayanagi[d], Manabu Akita[e], Takeshi Morimoto[d], and Zen Kawasaki[f]

[a]Centre of Technology for Disaster Risk Reduction (CDR), Fakulti Teknologi dan Kejuruteraan Elektronik dan Komputer (FTKEK), Universiti Teknikal Malaysia Melaka (UTEM), 76100 Durian Tunggal, Melaka, Malaysia
[b]Centre for Telecommunication Research and Innovation (CeTRI), Fakulti Teknologi dan Kejuruteraan Elektronik dan Komputer (FTKEK), Universiti Teknikal Malaysia Melaka (UTEM), 76100 Durian Tunggal, Melaka, Malaysia
[c]Institute of Energy Infrastruture, Universiti Tenaga Nasional, Selangor, Malaysia
[d]Department of Electrical, Electronic and Communication Engineering, Kindai University, Osaka, Japan
[e] University of Electro-Communication (UEC), Tokyo, Japan
[f]Graduate School of Engineering, Osaka University, Osaka 565-0871, Japan

Abstract

Narrow bipolar events (NBEs) generate strong radio emissions. In this paper, spatio-temporal analysis of 15 NBEs recorded from a tropical storm over Sumatra Island is presented. Two localization systems, namely the magnetic direction finder (MDF) and interferometer (ITF), were employed and utilized to get 2D mapping of the analysed NBEs. A total of four positive NBEs (+NBEs) and 11 negative NBEs (-NBEs) have been identified. The emission heights for +NBEs ranged from 8.38 km to 13.21 km, while for -NBEs, the emission heights were localized and compact ranging between 15.43 km and 15.76 km. The emission distances for all NBEs fell within the range of 233.33 km to 243.87 km. The maximum cloud top height was estimated at 18.61 km. The upward movement of very high frequency (VHF) radiation sources has been observed for all four positive NBEs indicating fast negative breakdowns (FNBs).

1 Introduction

This study is part of Science and Technology Research Partnership for Sustainable Development (SATREPS) which is a five-year international collaborative project between Japan and Malaysia universities with the title “real-time lightning 3D imaging and forecasting project for sustainable and reliable supply of energy and storm disaster early warning" started on 11 June 2023. The main institutions involved in this project are Kindai University in Japan, Univeriti Teknikal Malaysia Melaka (UTeM), and Universiti Tenaga Nasional (UNITEN) in Malaysia [1].

Lightning detection methods have evolved significantly, with various techniques and systems being developed for accurate and reliable detection. Researchers have explored the effectiveness of lightning detection systems using Bayesian approaches, comparing the probability of detection between different systems [2]. Additionally, the Asia-Pacific Lightning Location Network (APLLN) has been developed, assuming that lightning travels to each site in the form of a direct wave with a propagation speed of approximately the speed of light [3]. This network has provided valuable insights into lightning detection and positioning.

Various electromagnetic radio frequency-based lightning locating techniques, such as magnetic direction finder (MDF), time of arrival, and interferometer (ITF), have been employed for lightning mapping [4]. Furthermore, the feasibility of long-range lightning location networks with equivalent propagation velocity has been verified through comparisons with existing lightning locating systems [5]. These advancements have contributed to the development of more reliable lightning detection methods.

Lightning mapping using very high frequency (VHF) ITFs with cross-correlation two-dimensional (2D) mapping techniques has been a subject of interest in recent research. The use of VHF radiation (60–66 MHz) emitted during electrical breakdown has enabled the estimation of total lightning flash rates and the mapping of individual flash locations and sizes [6]. It utilizes the feature that electromagnetic waves associated with lightning discharges are broadband and employs interferometry over a wide band with the same principles as for a narrow-band signal [7]. This technique has been used to map negative cloud-to-ground lightning flashes, reporting 2D progression speeds for dart leaders and dart-stepped leaders [8]. Additionally, it has been combined with three-dimensional Lightning Mapping Array (LMA) observations to produce quasi-3D maps of lightning activity with high time resolution [9].

Furthermore, the study of lightning physics on scales exceeding the line-of-sight domains of ground-based VHF band LMAs has been facilitated by the use of ITF/optical whole sky systems [10]. The correlation between the charge structure evolution and lightning type and frequency has been analysed using observations from a three-dimensional lightning VHF radiation source location system, providing insights into the evolution of charge structure and lightning discharge characteristics [11].

Narrow Bipolar Events (NBEs) are impulsive and powerful radio emissions from intracloud discharges characterized by intense VHF radiation, fast propagation speed, and

978-3-8007-6416-7/24/$31.00 ©2024 IEEE

short-duration bipolar sferic waveforms in the low frequency band [5]. Recent studies have shed light on the initiation processes of NBEs, revealing the involvement of a relatively unknown type of discharge called fast positive breakdown (FPB) [12][13]. Additionally, it has been suggested that fast breakdown (FB), which can be either positive or negative in polarity, is responsible for the generation of NBEs [14][15]. These FB processes propagate at velocities comparable to or faster than laboratory-produced streamers and exhibit complex behaviour, producing opposite polarity breakdown that travels backward along the same path as the original discharge [15].

Furthermore, observations have indicated that NBEs can be associated with blue optical flashes on cloud tops, which have been attributed to extensive streamer electrical discharges [14]. The association between NBEs and blue discharges suggests the involvement of streamer coronas in the generation of NBEs [14]. Moreover, it has been demonstrated that NBEs can initiate normal intra-cloud (IC) lightning, highlighting their significance in the overall lightning activity within thunderstorms [15].

In this paper, motivated by the finding in [16], we analysed the emission distance and height of NBEs from the FA waveform based on the NBEs ionosphere reflection [17]. The MDF system is used to locate the azimuth angle of the NBEs from the MDF station whereas the ITF system is used the analysed the FB of NBEs VHF radiation to determine whether it is a FPB or fast negative breakdown (FNB). From this analysis we can locate the NBEs location, and we can evaluate the height of the NBEs with the cloud-top satellite imagery (HIMAWARI-9 L1B IR1 4k).

2 Methodology

The MDF and ITF systems are situated at a location within Universiti Teknikal Malaysia Melaka (UTeM) (2°18'50.14" N, 102°19'6.6" E), specifically on the rooftop of the Faculty of Electronics and Computer Technology and Engineering (FTKEK) laboratory. The system was set up on December 29th, 2023, and data collection has been ongoing up to the present day. The ITF setup is marked as the first installation of the equipment from Japan in Malaysia as part of the activity in the SATREPS project [1].

This system comprises a fast antenna (FA) sensor coupled with a single-station magnetic field sensor. The fast-varying electric field measurement employs wideband antennas with parallel plate configurations made from circular aluminium plates. Upon reaching the predetermined trigger level, the waveforms of the lightning event are automatically saved for subsequent analysis.

The FA is connected to both the MDF and ITF systems, where MDF consists of a pair of orthogonal wideband magnetic field antennas (additional details can be found in [18] and broadband ITF. **Figure 1** illustrates the schematic diagram of the MDF and ITF system setup. Radar echo (CAPPI format at 2 km altitude) and cloud-top satellite imagery (HIMAWARI-9 L1B IR1 4k) used here have been obtained from the Malaysia Meteorological Department (MMD).

The output of the wideband electric field antenna, orthogonal wideband magnetic field antennas, and broadband ITF antenna was digitized using two digitizers. For orthogonal wideband magnetic field antennas, the output is digitized with a resolution of 12 bits, and the data records were event-triggered, lasting 2 seconds. Meanwhile, for the broadband interferometer, digitization occurs with an 8-bit resolution, and the data record spans 100 milliseconds.

The timing for each event was provided by a Global Positioning System (GPS) with an accuracy of ±6 ns. Additional details of the E-field instrumentation are provided in [21]. The observations presented here were obtained from a single storm that formed on January 16, 2024. The time used in this paper is local Malaysian time with UTC+8.

The ITF comprises three resistively coupled flat-plate antennas arranged to form two equal-length orthogonal baselines. In this system, the antenna separation was 15 m in two perpendicular directions, and the received signals were band-limited to 20–80 MHz before digitization. A summary of the ITF's attributes is provided in the table below.

Due to limitations in rooftop space, the maximum baseline length for the ITF is set at 15 meters. The ITF is oriented in the North-South direction but is rotated 217° from North as an offset value, as illustrated in **Figure 2**. The numbered circle in the **Figure 2** represents the VHF antenna number, and azimuth calculations are dependent on the rotated value.

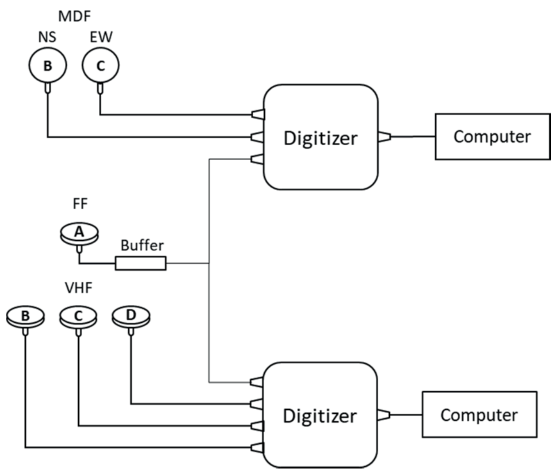

Figure 1 MDF and ITF schematic diagram

Table 1 Parameters for the ITF

ITF Parameters	
Number of antennas	3
Band Limited	20-80 MHz
Bandwidth	60 MHz
Center Frequency	50 MHz
Baseline	15 m
Sampling rate	250 MS s^{-1}
Resolutions	8 bits
Window	100 ms

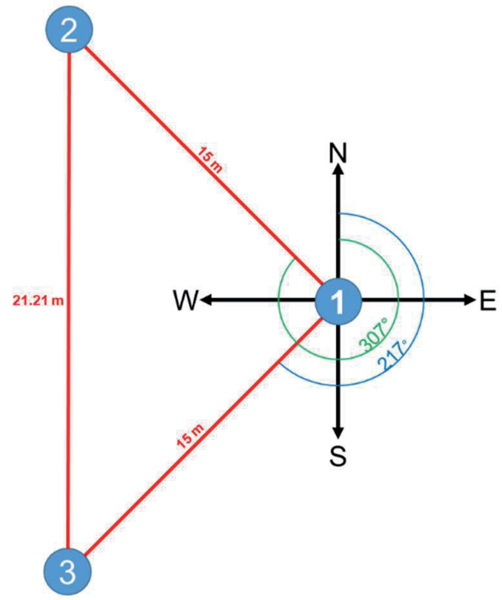

Figure 2 The offset rotation of the ITF relation to cardinal direction.

To determine the azimuth and elevation values of the ITF, equations (1) and (2) can be utilized, where τ_d1 represents the time delay between VHF 1 and VHF 2, τ_d2 is between VHF 1 and VHF 3, and c is the speed of light. The time differences τ_d1 and τ_d2 are calculated using the generalized cross-correlation technique [9], with values constrained to not exceed τ_transit = baseline/c. In post-processing, the VHF signal is up-sampled and divided into 2.05µs windows, with successive windows overlapped by 32ns.

$$Azimuth = arctan\left(\frac{\tau_{d1}}{\tau_{d2}}\right) \quad (1)$$

$$Elevation = arccos\left(\frac{c}{baseline}\sqrt{\tau_{d1}^2 + \tau_{d2}^2}\right) \quad (2)$$

In this study, the NBE reflection was visible, allowing us to calculate the estimation of the distance (d) and height (h) based on a flat Earth propagation model, as employed in [17]. The calculations are governed by the following equations:

$$\sqrt{d^2 + (2H - h)^2} - \sqrt{d^2 + h^2} = t_1 c \quad (3)$$

$$\sqrt{d^2 + (2H + h)^2} - \sqrt{d^2 + h^2} = t_2 c \quad (4)$$

In these equations, H represents the ionospheric virtual height estimate (86 km during night time), c denotes the speed of light, and t_1 and t_2 stand for the differential delays attributed to ionospheric and ground ionospheric reflections (see **Figure 3**), respectively. These equations were simultaneously solved using a minimum mean square error technique.

3 Result and Analysis

In this study, 15 NBE samples with ionosphere reflection were collected, comprising 4 +NBEs and 11 -NBEs. One field record of a +NBE (record number 1288; the first +NBE out of the total 15 detected +NBEs) is illustrated in **Figures 3 and 4**. This specific +NBE was located at a distance of 233.33 km from the observation station, with the emission's height measured at 8.38 km above mean sea level (msl).

Figure 4 illustrates the overlay image of Cappi radar echo (see **Figure 4(a)**) and Himawari cloud-top satellite imagery (see **Figure 4(b)**). In this study, we used Himawari cloud-top height image as our temperature-to-height reference for the tropical region [21].

As depicted in **Figure 5**, the first +NBEs occurred at 03:39:38, and 25 minutes later, the second +NBE was detected. The heights for the first and second +NBE were 8.38 km and 9.07 km above msl, with distances of 233.33 km and 238.11 km, respectively.

At 04:07:56, the first -NBE from a total of 8 -NBEs detected and within 3 minutes the rest were detected. The emission heights ranging between 15.43 km and 15.70 km above msl and maximum horizontal separations between the -NBEs were between 242.11 km and 243.87 km.

After 40 minutes, another two +NBEs were detected with higher emission heights than the previous +NBEs, between 10.78 km and 13.21 km above msl and distances between 260.97 km and 267.84 km. Subsequently, another three -NBEs detected with emission heights like the previous -NBEs, which were between 15.48 km and 15.76 km above msl.

Figures 6 and **Figure 7** shows the azimuth and elevation angle for the first detected +NBE from ITF system. From the initiation point, the upward movement of the VHF radiation sources indicates the occurrence of FNB rather than FPB [21]. A similar scenario was documented in [13], wherein a +NBE was associated with FNB instead of FPB.

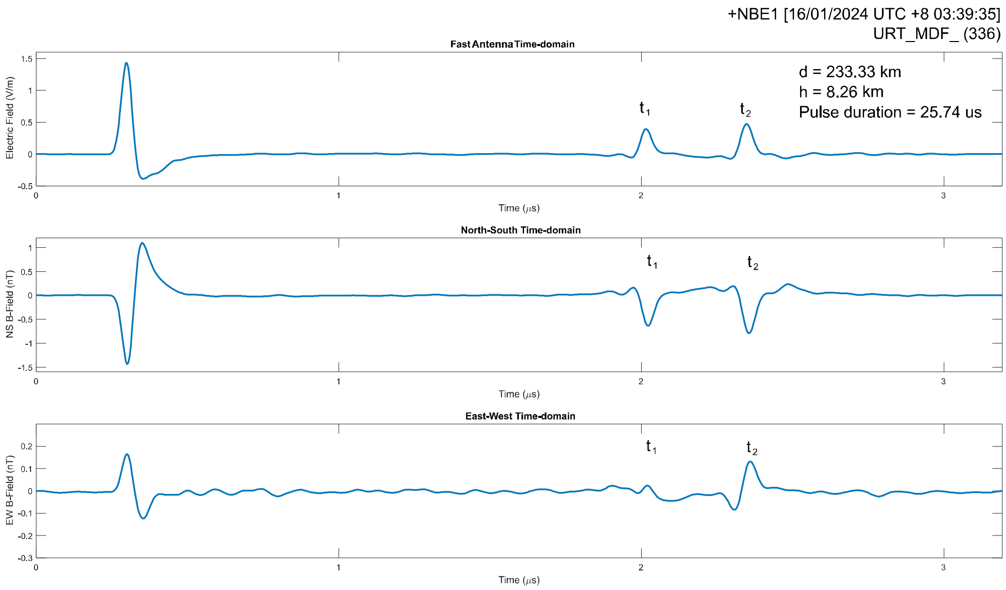

Figure 3 Wideband electric and magnetic radiation fields from a positive NBE (+NBE) at a distance d = 233.33 km from the observation station with height h = 8.26 km above MSL. The pulse duration for the NBE is 25.84 us. The ionospheric and ground-ionospheric reflections are shown as t_1 and t_2, respectively.

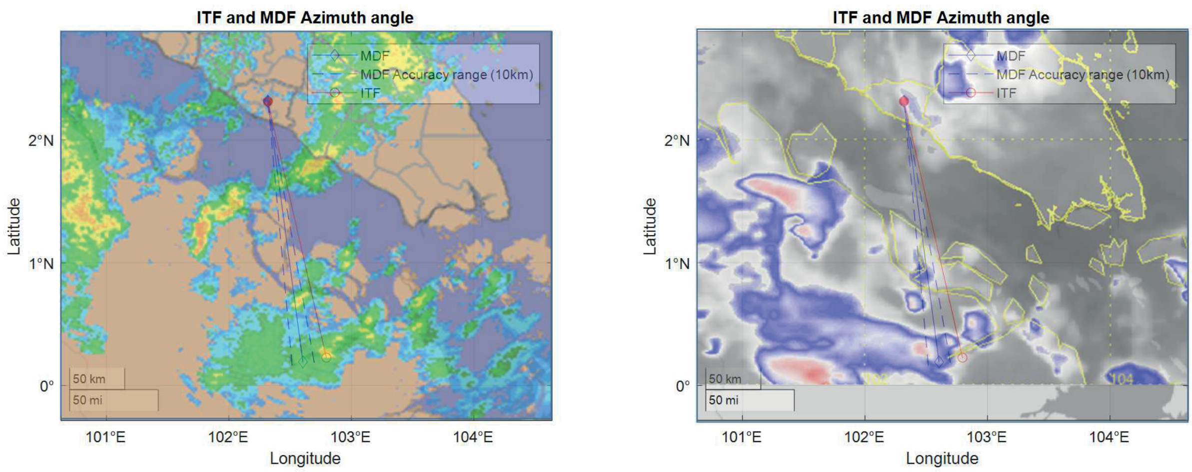

(a) (b)

Figure 4 The MDF azimuth (blue line) with 10 km range accuracy with ITF azimuth (red line) as comparison and distance of the +NBE occurred in data record number 1289 overlay with (a) Cappi radar echo and (b) Himawari cloud-top satellite image.

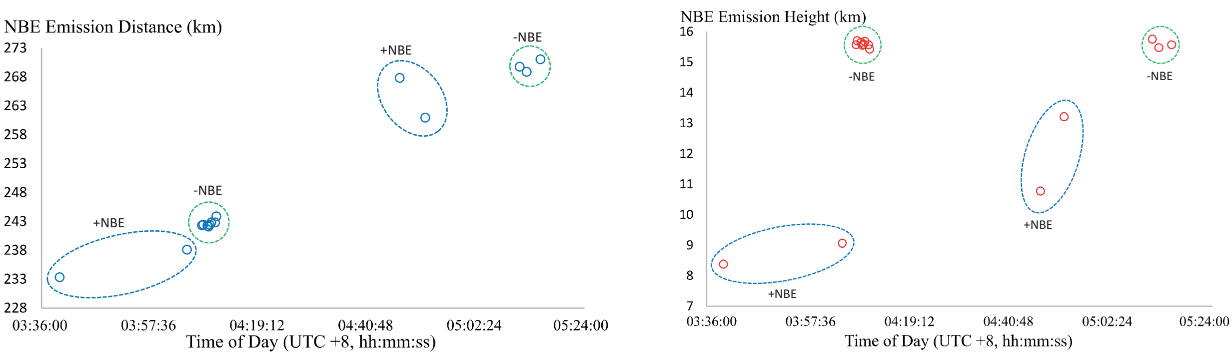

(a) (b)

Figure 5 (a) NBE emission distance with local time (UTC +8) and (b) NBE emission height with local time (UTC +8) where the +NBE were marked with blue dotted circle and the –NBE were marked with green dotted circle.

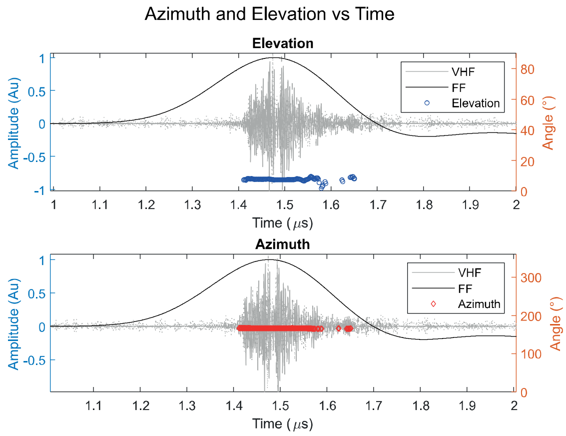

Figure 6 : The ITF mapping for +NBE1 showing the breakdown. The blue marker is the elevation whereas the red marker is azimuth angle. Radiation of the FA records (black waveform) was superimposed on the VHF radiation (gray waveform)

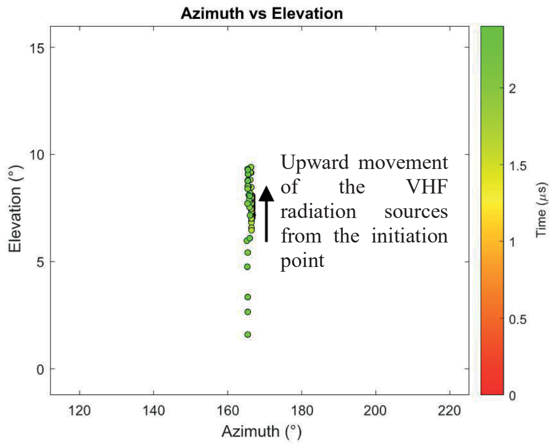

Figure 7 : The 2D maping of the VHF radiation sources with color maker as time range.

4 Conclusion

In this paper, we present findings on the emission height and distance of NBEs originating from a tropical thunderstorm. There are 4 +NBEs and 11 -NBEs observed during the 95-minute duration of the thunderstorm. The emission height ranges from 8.38 km to 15.70 km above mean sea level (MSL), with the emission distance spanning from 233.33 km to 243.87 km. Specifically, for +NBEs, the height varies from 8.38 km to 13.21 km above MSL, while -NBEs exhibit emission heights ranging from 15.43 km to 15.76 km above MSL. Notably, the -NBEs occur multiple times in a short period. The cloud-top height for the thunderstorm is estimated at 18.61 km maximum. Regarding the ITF system, the 2D mapping of +NBE1 reveals an upward movement from the initial point, indicating FNB.

5 Acknowledgement

This research work is supported by SATREPS (GERAN ANTARABANGSA-SATREPS/2023/FKEKK/A00052, A00046, A00043, and A00050) in collaboration between Japan Science and Technology Agency (JST, JPMJSA2210) and JICA. It is also promoted by Ministry of Higher Education (MOHE) in Malaysia. The authors express their gratitude to Universiti Teknikal Malaysia Melaka, Universiti Tenaga Nasional, and Kindai University for their collaboration and support.

6 References

[1] Morimoto, T. *et al.* (2023) 'Real-time lightning 3D imaging and forecasting project for sustainable and reliable supply of energy and storm disaster early warning "SATREPS project in Malaysia"', *Proceedings of the XXXVth URSI General Assembly and Scientific Symposium – GASS 2023* [Preprint]. doi:10.46620/ursigass.2023.1244.byib1995.

[2] Rison, W., Krehbiel, P., Stock, M., Edens, H., Shao, X., Thomas, R., … & Yang, Z. (2016). Observations of narrow bipolar events reveal how lightning is initiated in thunderstorms. Nature Communications, 7(1). https://doi.org/10.1038/ncomms10721

[3] Wang, J., Huang, Q., Ma, Q., Chang, S., He, J., Wang, H., … & Gao, C. (2020). Classification of vlf/lf lightning signals using sensors and deep learning methods. Sensors, 20(4), 1030. https://doi.org/10.3390/s20041030

[4] Alammari, A., Alkahtani, A., Ahmad, M., Noman, F., Esa, M., Kawasaki, Z., … & Tiong, S. (2020). Lightning mapping: techniques, challenges, and opportunities. Ieee Access, 8, 190064-190082. https://doi.org/10.1109/access.2020.3031810

[5] Li, D., Luque, A., Gordillo-Vázquez, F., Silva, C., Krehbiel, P., Rachidi, F., … & Rubinstein, M. (2022). Secondary fast breakdown in narrow bipolar events. Geophysical Research Letters, 49(7). https://doi.org/10.1029/2021gl097452

[6] Basarab, B. & Rutledge, S.A. & Fuchs, B.. (2015). An improved lightning flash rate parameterization developed from Colorado DC3 thunderstorm data for use in cloud-resolving chemical transport models. Journal of Geophysical Research: Atmospheres. 120. 10.1002/2015JD023470.

[7] Takayanagi, Y., Akita, M., Nakamura, Y., Yoshida, S., Morimoto, T., Ushio, T., … & Yamamoto, K. (2013). Development of vlf/lf bands interferometer and its initial observations. Electrical Engineering in Japan, 185(4), 9-17. https://doi.org/10.1002/eej.22300

[8] Sun, Z. *et al.* (2014) 'Characteristics of a rocket-triggered lightning flash with large stroke number and the associated leader propagation', *Journal of Geophysical Research: Atmospheres*, 119(23). doi:10.1002/2014jd022100.

[9] Stock, M., Akita, M., Krehbiel, P., Rison, W., Edens, H., & Kawasaki, Z. (2014). Continuous broadband digital interferometry of lightning using a generalized cross-correlation algorithm. Journal of Geophysical Research Atmospheres, 119(6), 3134-3165. https://doi.org/10.1002/2013jd020217

[10] Peterson, M., Rudlosky, S., & Deierling, W. (2018). Mapping the lateral development of lightning flashes from orbit. Journal of Geophysical Research Atmospheres, 123(17), 9674-9687. https://doi.org/10.1029/2018jd028583

[11] Li, D., Luque, A., Gordillo-Vázquez, F., Liu, F., Lu, G., Neubert, T., … & Reglero, V. (2021). Blue flashes as counterparts to narrow bipolar events: the optical signal of shallow in-cloud discharges. Journal of Geophysical Research Atmospheres, 126(13). https://doi.org/10.1029/2021jd035013

[12] Rison, W., Krehbiel, P., Stock, M., Edens, H., Shao, X., Thomas, R., … & Yang, Z. (2016). Observations of narrow bipolar events reveal how lightning is initiated in thunderstorms. Nature Communications, 7(1). https://doi.org/10.1038/ncomms10721

[13] Tilles, J., Liu, N., Stanley, M., Krehbiel, P., Rison, W., Stock, M., … & Wilson, J. (2019). Fast negative breakdown in thunderstorms. Nature Communications, 10(1). https://doi.org/10.1038/s41467-019-09621-z

[14] Liu, F., Zhu, B., Lu, G., Qin, Z., Lei, J., Peng, K., … & Zhou, H. (2018). Observations of blue discharges associated with negative narrow bipolar events in active deep convection. Geophysical Research Letters, 45(6), 2842-2851. https://doi.org/10.1002/2017gl076207

[15] Soler, S., Pérez-Invernón, F., Gordillo-Vázquez, F., Luque, A., Li, D., Malagón-Romero, A., … & Østgaard, N. (2020). Blue optical observations of narrow bipolar events by asim suggest corona streamer activity in thunderstorms. Journal of Geophysical Research Atmospheres, 125(16). https://doi.org/10.1029/2020jd032708

[16] Ahmad, M.R. et al. (2017) 'Emission heights of narrow bipolar events in a tropical storm over the Malacca Strait', 2017 International Conference on Electrical Engineering and Computer Science (ICECOS) [Preprint]. doi:10.1109/icecos.2017.8167155.

[17] Smith, D.A., Shao, X.M., Holden, D.N., Rhodes, C.T., Brook, M., Krehbiel, P.R., Stanley, M., Rison, W., Thomas, R.J., 1999. A distinct class of isolated intracloud lightning discharges and their associated radio emissions. J. Geophys. Res. 104, 4189–4212.

[18] Lu, G., R. Jiang, X. Qie, H. Zhang, Z. Sun, M. Liu, Z. Wang, and K. Liu (2014), Burst of intracloud current pulses during the initial continuous current of a rocket-triggered lightning flash, Geophys. Res. Lett., doi:10.1002/2014GL062127.

[19] Ahmad, M.R., Esa, M.R.M., Cooray, V., Dutkiewicz, E., 2014. Interference from cloud-to-ground and cloud flashes in wireless communication system. Electr. Power Syst. Res. 113, 237–246.

[20] Connolly, Michael & Connolly, Ronan. (2014). The physics of the Earth's atmosphere II. Multimerization of atmospheric gases above the troposphere. 10.13140/RG.2.2.26044.16003.

[21] Baharin, S.A. *et al.* (2022) 'Microwave radiation associated with positive narrow bipolar events', *SSRN Electronic Journal* [Preprint]. doi:10.2139/ssrn.4165802.